



Published in final edited form as:

Nat Immunol. 2018 December ; 19(12): 1309–1318. doi:10.1038/s41590-018-0243-7.

Autocrine-Paracrine Prostaglandin E₂ Signaling Restricts TLR4 internalization and TRIF Signaling

Darren J. Perkins¹, Katharina Richard¹, Anne-Marie Hansen¹, Wendy Lai¹, Shreeram Nallar¹, Beverly Koller², and Stefanie N. Vogel^{1,*}

¹Department of Microbiology and Immunology, University of Maryland, Baltimore (UMB), School of Medicine, 685 W. Baltimore St., Suite 380, Baltimore, MD

²Department of Genetics, UNC School of Medicine, Chapel Hill, NC

Abstract

The unique cell biology of Toll-like receptor 4 (TLR4) allows it to initiate two signal transduction cascades: a Mal (TIRAP)–MyD88-dependent signal from the cell surface that regulates proinflammatory cytokines and a TRAM–TRIF-dependent signal from endosomes that drives type I interferon production. Negative feedback circuits to limit TLR4 signals from both locations are necessary to balance the inflammatory response. We describe a negative feedback loop driven by autocrine-paracrine prostaglandin E₂ (PGE₂), and the PGE₂ receptor, EP4, which restricted TRIF-dependent signals and IFN- β induction through regulation of TLR4 trafficking. Inhibition of PGE₂ production or EP4 antagonism increased the rate of TLR4 endosomal translocation, and amplified TRIF-dependent IRF3 and caspase 8 activation. This PGE₂-driven mechanism restricted TLR4-TRIF signaling *in vitro* upon infection of macrophages by Gram-negative pathogens *Escherichia coli* and *Citrobacter rodentium* and protected mice against *Salmonella enteritidis* serovar Typhimurium (ST)-induced mortality. Thus, PGE₂ restricts TLR4-TRIF signaling specifically in response to lipopolysaccharide.

Keywords

PGE₂; TRIF; IFN- β ; TLR4; EP4; macrophages

Users may view, print, copy, and download text and data-mine the content in such documents, for the purposes of academic research, subject always to the full Conditions of use:http://www.nature.com/authors/editorial_policies/license.html#terms

*Corresponding Authors: Stefanie Vogel, svogel@som.umaryland.edu, and Darren Perkins dperkins@som.umaryland.edu, Ph: 410-706-4838, FAX: 410-706-8607.

Author Contributions

D.J.P and S.N.V. conceived the study, designed the experiments, and wrote the manuscript. D.J.P performed the majority of the experiments. K.R. performed TLR4 translocation experiments. A.M.H performed *E. coli* and *C. rodentium* infections, W.L. performed IFN- β ELISAs, and analyzed the data. S.N. bred and genotyped all mice with targeted mutations. B.K. developed, bred, genotyped, and isolated femurs from *Ptger4*^{-/-} and littermate control mouse strains.

Data Availability

Microarray data associated with Figure 1 has been deposited within GEO database #GSE111826. The data that support the findings of this study are available from the corresponding author upon request.

Competing Interests

The authors declare they have no competing interests.

Introduction

The host innate immune inflammatory response to Gram-negative bacterial lipopolysaccharide (LPS) is mediated by Toll-like receptor 4 (TLR4) recognition of LPS in the context of TLR4-bound MD2^{1, 2, 3}. TLR4 is unique among the TLRs in that following recognition of LPS by MD2, two separate “modes” of signaling can be initiated, each from a distinct cellular compartment that utilizes distinct signaling intermediates, resulting in discrete transcriptional programs⁴. Cell surface TLR4 engages intracellular adaptors TIRAP(Mal) and MyD88 through TIR domain interactions to activate NF- κ B and MAPK signaling and subsequent proinflammatory cytokine gene transcription (*e.g.*, *Tnf* and *Il1b*)⁵. A qualitatively distinct signal transduction cascade is elicited following endosomal translocation of a portion of LPS-bound TLR4-MD2 through an incompletely understood action of the cell surface co-receptor CD14^{6, 7, 8}. The TIR domain of endosomal TLR4 engages the adaptor TRAM which recruits the adaptor TRIF and activation of TBK-1 kinase that leads to phosphorylation of the transcription factor IRF3 and, ultimately, type I interferon (IFN) production (*e.g.*, IFN- β)^{9, 10, 11, 12}. In addition, TRIF signaling also activates a second, unique pathway involving caspase 8 and the RIP kinases 1 and 3 leading to caspase 1-independent processing of pro-interleukin 1 β (IL-1 β)^{13, 14, 15}. The kinetics of activation and termination of the separate signal transduction cascades driven by MyD88 and TRIF are necessarily limited to protect host tissues from excessive inflammation and to re-establish homeostasis. While MyD88-dependent cytokine production is crucial to clearing many bacterial infections¹⁶, conversely, the production of type I IFNs can promote infection in a number of models by a mechanism that involves a poorly understood immunosuppression^{17, 18, 19, 20, 21}. Thus, it is crucial to understand the molecular mechanisms that limit the inflammatory response and establish the balance between TLR4-MyD88 and TLR4-TRIF signaling.

A detailed understanding exists for how MyD88-dependent signaling kinetics are regulated. MyD88-driven NF- κ B rapidly drives expression of the A20 enzyme that accumulates and causes disassembly of the NF- κ B and MAPK signalosomes through de-ubiquitinase, as well as ubiquitin ligase, activities^{22, 23}. The negative feedback loop mediated by A20 induction is critical to host homeostasis as A20-deficient mice succumb to massive inflammation shortly after birth and A20-deficient macrophages display prolonged MyD88 signaling with enhanced NF- κ B and MAPK responses²⁴. Importantly, however, macrophages deficient in A20 display normal regulation of LPS-driven IRF3 activation, indicating that a distinct feedback loop regulates the TLR4/TRIF pathway²⁴.

Endogenously produced prostaglandin E₂ (PGE₂) is a strong candidate to inhibit TLR4-dependent IFN production due to its rapid synthesis and secretion in response to LPS^{25, 26}, autocrine mode of action²⁷, as well as its noted immunomodulatory capacity during Gram-negative infection²⁸. Additionally, PGE₂ has also been shown to display a reciprocally antagonistic pattern of expression with IFN- α/β in some bacterial infection models²⁹. PGE₂ itself is a secreted, bioactive, signaling lipid, frequently acting in an autocrine-paracrine manner, that can influence both inflammatory and homeostatic processes^{30, 31}.

In search of possible endogenous regulatory circuits that limit TLR4-TRIF-dependent IFN- β production during the response to Gram-negative LPS, we performed a microarray analysis of differential gene expression in wild-type *versus Ifnb*^{-/-} primary murine thioglycollate-elicited peritoneal macrophages (TEPMs) infected with *Salmonella enteritidis* serovar Typhimurium (*ST*). Subsequent bioinformatics analysis of those data predicted transcriptional regulators whose activities were inversely related to IFN- β expression during *ST* infection and identified the prostaglandin PGE₂-specific receptor EP4. We report herein that in response to bacterial LPS, PGE₂ was rapidly released from murine macrophages and participated in an autocrine-paracrine regulatory loop through the high-affinity PGE₂ receptor EP4. This PGE₂-EP4 signaling axis specifically limited the TRIF-dependent arm of the TLR4 response to LPS and thereby reduced type I IFN production, as well as the TRIF-dependent, caspase 1-independent, processing of IL-1 β . These findings contribute to our understanding of the regulation of endosomal TLR4 signals, as well as how type I IFN production during bacterial infections may be limited by the host.

Results

LPS-dependent PGE₂ limits IFN- β production.

We initially carried out a microarray analysis to identify transcripts whose induction by *ST* infection in macrophages was increased or inhibited specifically by IFN- β expression (wild-type *vs. Ifnb*^{-/-}). With these data, we utilized the Upstream Regulator Analytic within the Ingenuity Pathway Assist software to identify transcriptional regulators whose activity was predicted to be elevated or inhibited by IFN- β during the response to *ST*. As expected, this analysis identified a number of known regulators of type I IFN production or signaling as being inhibited in the absence of IFN- β expression (Fig. 1a). Notably, this analysis also predicted that the prostaglandin E₂ (PGE₂)-specific receptor, EP4, displayed activity which was inversely related to IFN- β production during the early (6 h) inflammatory response to *ST* infection, a time-point at which the innate inflammatory response to *ST* is predominantly TLR4-dependent¹⁷.

To elucidate a possible role for autocrine or paracrine PGE₂ in the regulation of TLR4 signaling in response to LPS, we first determined the kinetics of endogenous PGE₂ production in LPS-stimulated peritoneal macrophages. Activation of the proximal enzyme in the PGE₂ biosynthetic cascade, the calcium-dependent phospholipase A2 (cPLA2), was examined by phospho-specific immunoblot analysis. LPS stimulation of murine peritoneal macrophages resulted in activation of cPLA2 within 30 min that terminated by 90 min (Fig. 1b). Quantitation of extracellular PGE₂ by ELISA indicated that secreted PGE₂ could be readily detected within 3 h of LPS stimulation and LPS-dependent PGE₂ release could be inhibited by a small molecule antagonist of the microsomal PGE₂ synthase (mPGES-1), the terminal enzyme in the PGE₂ biosynthetic cascade that is essential for LPS-induced PGE₂ production³² (Fig. 1c). Analysis of secreted cytokine concentrations in supernatants of LPS-stimulated macrophages treated with vehicle (DMSO) or the mPGES antagonist revealed no effect of PGE₂ inhibition on TNF production; however, inhibition of PGE₂ production resulted in an increase in IFN- β secretion (Fig. 1d). This result was consistent with our preliminary hypothesis that autocrine-paracrine PGE₂ may negatively regulate the TLR4-

activated TRIF signaling pathway. Extracellular PGE₂ can be sensed by any of four specific PGE₂ receptors, EP1–4, each with distinct expression patterns and functions³³. We initially focused on a role for EP4 as it was identified in our bioinformatics analysis and had previously been implicated in regulating innate inflammatory responses³⁴. Therefore, macrophages were stimulated with LPS in the absence or presence of a specific, high-affinity EP4 antagonist. Treatment of cells with EP4 antagonist produced results identical to that seen with the mPGES antagonist with respect to enhanced production of IFN- β , with no effect on TNF secretion (Fig. 1e). Examination of additional MyD88-dependent (*i.e.*, A20) and IFN- β -dependent (*i.e.*, PKR) non-secreted proteins confirmed this pattern of regulation (Supplementary Fig. 1). In contrast to the increased production of IFN- β seen in LPS-stimulated macrophages treated with the EP4 antagonist, no enhancement of LPS-induced IFN- β was observed in the presence of specific antagonists for other PGE₂ receptors, EP2 or EP3 (Fig. 1f). To determine if inhibition of PGE₂ sensing by EP4 regulated *Ifnb* transcription, we measured *Tnf* and *Ifnb* mRNA over a 6 h time course of LPS stimulation, without or with EP4 antagonist. Selective blockade of the EP4 receptor enhanced transcription of LPS-induced *Ifnb* mRNA, but not *Tnf* mRNA (Fig. 1g). To confirm a role for EP4 in regulating LPS-induced IFN- β , bone marrow-derived macrophages (BMDMs) were generated from wild-type and *Ptger4*^{-/-} (EP4-null) mice and compared their production of LPS-induced IFN- β protein. *Ptger4*^{-/-} BMDMs produced significantly more IFN- β than wild-type BMDMs (Fig. 1h). These data indicated a role for endogenously produced PGE₂ in the selective suppression of IFN- β production in response to LPS.

Inhibition of PGE₂-EP4 enhances IRF3 activation

To explore the mechanism underlying the selective suppression of IFN- β production by PGE₂-EP4 during the response to LPS, we examined activation of the TRIF-activated transcription factor, IRF3, over a 180 min time course. In vehicle-treated, LPS-stimulated macrophages, IRF3 activation (p-IRF3) was observed between 60 and 120 min post-stimulation in agreement with previous work³⁵. However, in the presence of the specific EP4 antagonist, we observed enhanced amplitude and duration of IRF3 activation (Fig. 2a). In the presence of the EP4 antagonist, enhanced LPS-dependent IRF3 activation was also observed in the human monocytic cell line, THP-1, and in primary human monocytes (Supplementary Fig. 2). To determine the extent to which EP4 antagonism might prolong IRF3 activation, we performed an extended time course of LPS stimulation and observed significant IRF3 phosphorylation as late as 5 h post-LPS stimulation in the presence of the EP4 antagonist (Fig. 2b). To determine the specificity of EP4 regulation for IRF3, LPS-dependent activation of the MAPKs were examined in the absence or presence of EP4 antagonist. Neither Jnk, Erk, nor p38 activation were modulated in LPS-stimulated macrophages by EP4 antagonist (Fig. 2c). Thus, the inhibitory effect of the PGE₂-EP4 signaling axis appears to be specific for TLR4-mediated TRIF signaling.

We additionally examined the effect of EP4 antagonism on I κ B α degradation in response to LPS. The early kinetics of I κ B α degradation was not affected by EP4 antagonism; however, we consistently observed a delay in the re-synthesis of I κ B α in the presence of the EP4 inhibitor (Fig. 2d). This delayed I κ B α re-synthesis is consistent with the results of a prior report demonstrating regulation of I κ B α re-synthesis by the TRIF pathway³⁶. To

corroborate the results obtained with the EP4 antagonist, we compared the time course of IRF3 activation in wild-type and *Ptger4*^{-/-} BMDMs. Consistent with the results of our inhibitor studies, IRF3 activation was extended in the LPS-stimulated *Ptger4*^{-/-} BMDMs (Fig. 2e). The specificity of the EP4 receptor in regulating IRF3 activation was confirmed by comparing the effects of the EP4 antagonist with EP2- and EP3-specific antagonists. Only EP4 inhibition enhanced and prolonged LPS-dependent IRF3 activation (Fig. 2f). To control for potential non-specific effects of our EP4 antagonist, we subsequently compared the effects of global PGE₂ inhibition by the mPGES antagonist on the activation of IRF3 (Fig. 2g) and the re-synthesis of IκBα (Fig. 2h). In both instances, inhibiting PGE₂ production globally recapitulated the effects of the EP4-specific antagonist. Finally, we sought to ascertain if it were possible to amplify the effects of the endogenous autocrine or paracrine PGE₂ regulatory loop by treating macrophage cultures with exogenous PGE₂. Addition to macrophage cultures of 1 μM PGE₂, concurrent with LPS stimulation, significantly suppressed IRF3 activation (Fig. 2i). These experiments indicated that endogenously produced PGE₂ regulates TLR4-dependent *ifnb* transcription by limiting IRF3 activation.

PGE₂-EP4 regulates TRIF activation

The significant effect of EP4 antagonism on TLR4-dependent activation of IRF3, an event known to be strictly dependent on the adaptor TRIF¹⁰, led us to speculate that PGE₂-EP4 may be targeting this adaptor pathway specifically. LPS-induced IRF3 activation was examined in wild-type and *Trif*^{-/-} peritoneal macrophages in the absence or presence of mPGES or EP4 antagonists. IRF3 activation following LPS stimulation was strictly TRIF-dependent, whether or not the mPGES antagonist was present (Fig. 3a). Notably, the impact of the mPGES and EP4 antagonists on LPS-induced IκBα re-synthesis was completely reversed in *Trif*^{-/-} macrophages, again supporting the notion that the PGE₂-EP4 axis specifically targets the TRIF signaling pathway in its regulation of TLR4 signaling (Fig. 3a).

The TRIF pathway is initiated by the CD14-dependent translocation of the TLR4-LPS-MD2 complex into an endosome where it recruits the adaptors TRAM and TRIF to the TLR4 TIR domain that is exposed to the cytosol⁶. We monitored TLR4 endosomal translocation by TLR4 cell surface staining and flow cytometry analysis. Unstimulated cells exhibited no internalization of TLR4 over the time monitored. However, antagonizing EP4 with either the EP4 antagonist (Fig. 3b) or treatment of macrophages with the mPGES antagonist (Supplementary Figure 3) resulted in a more rapid and greater LPS-induced loss of TLR4 from the cell surface compared to vehicle-treated control macrophages.

Little is known of the signaling determinants that permit CD14-dependent TLR4 endosomal translocation, but it has been shown that there is an absolute requirement for activation of the tyrosine kinase Syk in a CD14-dependent, but TLR4-independent, fashion³⁷. Therefore, LPS-induced Syk activation was assessed in the absence or presence of the EP4 antagonist. Antagonism of EP4 during LPS stimulation resulted in a more rapid and increased activation of Syk (Fig. 3c), consistent with the results of our TLR4 internalization experiments (Fig. 3b). To test further the hypothesis that PGE₂-EP4 feedback restricts TRIF signaling specifically, peritoneal macrophages were stimulated with Pam3Cys, a ligand for TLR2, a TLR that engages MyD88, but not TRIF. The addition of the mPGES antagonist did not

affect TLR2-dependent signaling nor did it result in TLR2-dependent IRF3 activation (Fig. 3d). We did not, however, observe an effect of the EP4 antagonist on IFN- β induction in response to TLR3 stimulation by poly I:C, likely due to the fact that poly I:C is a very weak inducer of PGE₂ release when compared with LPS (Supplementary Fig. 4). These experiments demonstrated that PGE₂ regulates the TLR4-TRIF pathway activation through trafficking, and that TRIF expression is required for PGE₂ regulation of TLR4 signaling.

PGE₂-EP4 restricts TRIF-dependent caspase 8 activation

While PGE₂ feedback through EP4 is capable of restricting TLR4-TRIF-dependent activation of the TBK-1-IRF3 pathway, The TLR4-TRIF complex is also capable of activating caspase-8, leading to limited IL-1 β processing. To determine whether this second TRIF-dependent pathway were sensitive to PGE₂, the effect of the EP4 antagonist on LPS-dependent caspase 8 activation was measured (Fig. 4a). Blockade of EP4 augmented TRIF-dependent caspase 8 activation, as evidenced by increased abundance of the cleavage product, caspase 8 p18, as well as enhanced p-IRF3, in LPS-stimulated wild-type macrophages. It has previously been reported that LPS stimulation of macrophages alone results in a low-level processing and release of mature IL-1 β in a manner that is TRIF- and caspase 8-dependent and caspase-1-independent^{13, 15}. We speculated that PGE₂ release may limit this TRIF-Caspase 8-dependent effect on IL-1 β . Antagonizing EP4 significantly enhanced LPS-dependent IL-1 β release in a TRIF-dependent fashion and in the absence of a second inflammasome-activating stimulus (Fig. 4b). Because activation of EP4 by exogenous PGE₂ has recently been shown to inhibit inflammasome NLRP3-dependent caspase 1 activation and IL-1 β processing in response to LPS and NLRP3 activators³⁴, we examined caspase 1 directly, but found no activation due to the presence of the EP4 antagonist (Fig. 4c). These results demonstrated that both of the known signal transduction pathways initiated by TLR4-TRIF are negatively regulated by PGE₂.

cAMP-dependent effectors are regulators of TRIF

Having established that signaling through the EP4 receptor is required to restrict TRIF-dependent signals downstream of TLR4, we sought to define EP4-activated pathways necessary for this effect. There are two well-defined G protein-activated signal transduction cascades downstream of EP4, the first leading to activation of phosphatidylinositol-3-OH kinase (PI(3)K) and protein kinase Akt, and the second activating an endogenous adenylate cyclase (AC) leading to cAMP accumulation and activation of the cAMP-dependent effectors protein kinase A (PKA) and the nucleotide exchange factor for small GTPases, EPAC³⁸ (Fig. 5a). While complete inhibition of basal and LPS-inducible Akt phosphorylation was achieved with the Akt antagonist, the Akt antagonist had no effect on LPS-dependent IRF3 activation (Fig. 5b). In contrast, inhibition of either of the cAMP-dependent effectors, PKA or EPAC, led to an increase in LPS-dependent IRF3 activation, suggesting that the AC-dependent pathway mediates EP4 effects (Fig. 5c,d). To assess directly the ability of cAMP to suppress TLR4-dependent IRF3 activation, we utilized recombinant AC toxin from *Bordetella pertussis* which rapidly catalyzes the production of cytosolic cAMP independent of host enzymes³⁹. Addition of *B. pertussis* AC toxin dose-dependently reduced TLR4-mediated IRF3 activation (Fig. 5e), in addition to slowing the

kinetics of TLR4 internalization (Fig. 5f). Thus, the inhibitory effects of EP4 on the TLR4-TRIF pathway are mediated by cAMP-dependent effectors.

PGE₂-EP4 regulates *in vitro* and *in vivo* infections

To determine whether the observed PGE₂-EP4 feedback may be important in restricting IRF3 activation during *in vitro* infection with live Gram-negative pathogens, peritoneal macrophages were infected with intracellular *ST* at a low multiplicity of infection (MOI = 4), in the absence or presence of the mPGES inhibitor, and IRF3 activation was examined 6 h later (Fig. 6a). In the absence of mPGES inhibitor, no detectable IRF3 activation was observed after infection with *ST*. Inhibition of PGE₂ synthesis, however, significantly increased IRF3 activation in response to *ST in vitro* (Fig. 6a). *ST* is an intracellular pathogen and presumably presents LPS to TLR4 during the entire course of infection. Therefore, we sought to determine whether EP4 was also active in restricting IRF3 activation following a 60 min incubation of macrophages with two extracellular, enteric *E. coli* strains, enterohemorrhagic *E. coli* (EHEC) and enteropathogenic *E. coli* (EPEC), or the murine extracellular enteric pathogen *Citrobacter rodentium* (MOI = 25) (Fig. 6b). As observed for *ST*, restriction of PGE₂ production by mPGES inhibition enhanced IRF3 activation following infection with enteropathogenic *E. coli*, enterohemorrhagic *E. coli*, and *C. rodentium*.

To confirm that the PGE₂-EP4 axis limits type I IFN production during *in vivo* infection by a Gram negative pathogen, C57BL/6J mice were infected with *ST*. Mice were pre-treated with a single i.p. injection of saline or EP4 antagonist (50 µg/mouse) 60 min prior to i.p. infection with *ST*. Eight hours after infection, mice were euthanized and the spleens and livers harvested for gene expression analysis. Animals that received the EP4 antagonist displayed significantly elevated *Ifnb* expression in the spleen (Fig. 6c), with a similar trend observed in the liver (data not shown). Consistent with our *in vitro* studies, the effects of the EP4 antagonist displayed gene specificity and did not alter *in vivo* expression of *Tnf* (Fig. 6c), but we did observe reduced *Il1b* mRNA (Fig. 6c) in agreement with a recent report of a role for PGE₂ in *Il1b* transcription⁴⁰. Analysis of *ST* colony forming units (CFU) in spleen failed to show differentially altered bacterial numbers in either group at this early time point (Fig. 6d). These results indicate that signaling via the PGE₂-EP4 axis is important in limiting IRF3 activation and IFN-β induction during Gram negative bacterial infections *in vitro* and *in vivo*. We and others have previously demonstrated that expression of type I interferons during *in vivo ST* infection can promote pathogenesis and increase mortality in mice^{17, 18, 41, 42}. We therefore hypothesized that *in vivo* administration of EP4 antagonists during systemic *ST* infection would result in increased mortality due, at least in part, to elevated IFN-β production. To determine the impact of EP4 antagonism on the course of *ST* infection, animals were infected with *ST* (1×10³ CFU i.p.), followed by twice daily injections of the EP4 antagonist or saline control. Animals receiving the EP4 antagonist succumbed more rapidly to infection (*P* = 0.001), consistent with a key role for PGE₂-EP4 in the host defense against *ST* (Fig. 6e). Our data is consistent with a model in which PGE₂ is rapidly released in response to TLR4 ligation by LPS and selectively suppresses TLR4-TRIF signal transduction by activating cAMP-dependent effectors to restrict TLR4 endosomal translocation (Supplementary Figure 6).

Discussion

Mechanisms that restrict TLR4-dependent cytokine production are critical to limiting inflammatory damage and speeding the return to host homeostasis. The unique cell biology of TLR4-dependent signaling requires that feedback mechanisms be in place to restrict both cell surface-initiated (MAL(TIRAP)-MyD88-dependent) and endosomal (TRAM-TRIF-dependent) signaling. While cell surface TLR4-MyD88-dependent signals activating NF- κ B and MAPK are subject to negative regulation by an A20 feedback circuit, A20 does not limit endosomal TLR4-TRIF activation of IRF3²⁴. A negative feedback loop restricting the TRIF complex has not been generally described; however, there are reports of other mechanisms that limit aspects of TRIF activity. The deubiquitinase DUBA has been shown to act to inhibit the K63 ubiquitin ligase TRAF3, an activity that limits TRIF-dependent IRF3 activation specifically⁴³. Additionally, it has been demonstrated that inflammasome activation of caspase 1 during some bacterial infections can cleave TRIF and thereby limit TRIF-dependent signaling⁴⁴; however, such a mechanism would only be operative in the presence of second signal to permit maturation of the inflammasome.

Our current observations are both novel and important because we describe for the first time the action of an autocrine or paracrine PGE₂-dependent feedback loop downstream of TLR4 activation by LPS that limits both the amplitude and duration of TRAM-TRIF-dependent signaling by restricting the CD14-dependent trafficking of TLR4-MD2 into endosomes necessary for the recruitment of TRAM-TRIF to the cytosolic Toll-IL-1R Resistance (TIR) domain. The biochemistry of PGE₂ makes it uniquely suited to serve in a feedback capacity to regulate TLR4 responses for two reasons: first, PGE₂ can be rapidly synthesized and released within minutes after TLR4 ligation, independent of *de novo* transcription and translation²⁵. Secondly, PGE₂ is an autocrine-acting factor with an extremely short life-span *in vivo* of less than 30 seconds⁴⁵ which would permit secreted PGE₂ to restrict TRIF signaling in a cell-autonomous manner with limited systemic effects, unlike a relatively long-lived protein cytokine.

While PGE₂ can be recognized by four distinct G-protein coupled receptors (EP1–4)³³, we identified the EP4 receptor, specifically, as mediating the actions of secreted PGE₂ against the TRIF pathway, and recent reports highlight a growing appreciation of the significance of EP4 in regulating inflammatory responses *in vitro* and *in vivo*^{34, 46}. While EP4 shares the greatest sequence and signaling similarity (including activating adenylate cyclase) with another PGE₂ receptor, EP2, the EP4 receptor has an affinity for PGE₂ that is ~7–8-fold greater than EP2⁴⁷, possibly making EP4 uniquely suited to sense and respond to the low autocrine or paracrine levels of PGE₂ secreted soon after TLR4 ligation. Importantly, while some previous *in vitro* studies have shown a broadly suppressive effect of PGE₂ against all TLR4-driven cytokine responses^{48, 49, 50}, such studies have typically relied upon relatively high levels of exogenously added PGE₂ that may simultaneously ligate multiple distinct PGE₂ receptors, producing a distinct regulatory outcome from the autocrine or paracrine loop described herein.

Our data also support the hypothesis that downstream of EP4, activation of endogenous AC enzymes and the generation of cAMP are important for the action of EP4 in restricting TRIF-mediated signaling. The identification of the cAMP-dependent effectors PKA and

EPAC in limiting TRIF-dependent IRF3 activation is intriguing in light of the effects of EP4 on TLR4 internalization. The movement of TLR4 from the cell surface to an early endosome compartment is essential for TRIF recruitment and IRF3 activation. While cell surface expression of CD14 is absolutely required for TLR4 to be internalized in response to LPS, whether the rate of TLR4 internalization is constant or is dynamic and subject to regulation has not been investigated. Our work represents the first report showing that the kinetics of TLR4 internalization are subject to regulation by the extracellular inflammatory milieu. In this regard, it is also notable that a ligand for TLR3, poly I:C, a receptor that does not require trafficking to engage TRIF and is not inhibited by the EP4 antagonist, elicits very little PGE₂ release when compared to LPS. While little detail is known about the molecular machinery that coordinates the trafficking of TLR4, TRAM, and TRIF to endosomes, it is clear that small GTPases are required and, specifically, Arf6 and Rab11a^{51, 52}. Both PKA and EPAC have been shown to negatively regulate endosomal trafficking by Rab family GTPases and Rab11a in response to cAMP-generating bacterial toxins^{53, 54, 55}. In this context, PKA and EPAC were shown to act synergistically, targeting different aspects of the Rab11-exocyst complex, thereby limiting early recycling endosome kinetics⁵⁶. Conceivably, a similar role for PKA and EPAC could operate in response to endogenously produced PGE₂ to limit TLR4-TRIF complex assembly. Further studies will be required to elucidate the precise inter-molecular interactions between the cAMP effectors and elements of the TLR4-TRIF pathway; however, a potential implication of this model is that the rate of CD14-dependent internalization of TLR4 may be responsive to and reflective of the local PGE₂ concentration.

Our current work has significant implications for understanding how the different modes of TLR4 signaling shape the outcome of bacterial infection. *In vivo*, establishing the balance between pro-inflammatory cytokines (TNF, IL-1 β , IL-6) and type I IFN is important in pathogenesis. Inflammatory cytokines are clearly needed to restrict bacterial growth and, ultimately, clear microbes¹⁶, while some coincident type I IFN production can be beneficial by limiting damage due to systemic inflammation⁵⁷. However, type I IFN production must be carefully regulated, as it has been shown in a number of other bacterial infection models that the suppressive effects of type I IFN promote bacterial growth and exacerbate disease^{17, 18, 21, 29, 42, 58, 59}. Therefore, striking a precise balance between TLR4-MyD88- and TLR4-TRIF-dependent outcomes is likely key in re-establishing homeostasis. Our data support the concept that the PGE₂-EP4 axis is an important conduit of cross-talk between the two signaling pathways.

Methods

Animals and Cells

Animal work performed for this study complied with all applicable provisions of the Animal Welfare Act; U.S. Government Principles for the Utilization and Care of Vertebrate Animals Used in Testing, Research, and Training; Public Health Services Policy on the Humane Care and Use of Laboratory Animals; and Guide for the Care and Use of Laboratory Animals (8th edition). The protocol for this work was approved by the Institutional Animal Care and Use Committee of the University of Maryland, School of Medicine. Primary thioglycollate-

elicited peritoneal macrophages (TEPMs) were prepared as described previously⁶⁰. Briefly, 3 ml of 3% sterile thioglycollate (Remel) was injected i.p into 6–8 week old, wild-type C57BL/6J mice (Jackson Laboratories). Four days later, macrophages were harvested by peritoneal lavage with sterile saline. TRIF-null mice (*Trif*^{-/-}), backcrossed onto a C57BL/6J background (*n* = 10), were bred in-house as described previously⁶¹. Femurs from *Ptger4*^{-/-} (EP4-deficient) and littermate *Ptger4*^{+/+} control mice^{62, 63} were used to generate BMDMs as described previously⁶⁴. The human THP-1 cells were plated at 2×10^6 cells per well and treated with 100 nM phorbol 12-myristate 13 acetate (PMA) for 48 h after which the cells were washed and the PMA removed. Cells were allowed to rest for an additional 24 h prior to LPS stimulation. Human monocytes were isolated from whole blood by counter flow centrifugal elutriation from PBMCs that were obtained from blood of healthy human volunteers at the Department of Transfusion Medicine, National Institutes of Health (NIH; kindly provided by L. Wahl, National Institute of Dental and Craniofacial Research, NIH). Elutriated monocytes were plated for 2 h in serum-free medium (DMEM +1 % penicillin-streptomycin, 1% L -glutamine). Human AB-positive serum (2.5%; Gemini Bio-Products) was added after 2 h. Monocytes were allowed to rest overnight before stimulation with LPS (100 ng/ml) without or with EP4 antagonist (50 μ M) (Tocris Bioscience).

Antibodies and Reagents

Antibodies against cPLA2 (D49A7), phospho-cPLA2 (D4I2A), IRF3 (D83B9), phospho-IRF3(4D4G), phospho-TBK-1 (D52C2), phospho-JNK (81E11), phospho-ERK1/2 (D13.14.4E), p38 (D13E1), phospho-p38 (D3F9), I κ B α (44D4 and 9242), Syk (2712), phospho-Syk TYR525/526 (C87C1), AKT (11E7), and phospho-AKT Ser473 c(D9E) were obtained from Cell Signaling. Anti-Caspase-1 p20 was obtained from Adipogen. Protein-free phenol/water-extracted *Escherichia-coli* K235 LPS was prepared as described previously⁶⁵. S-[2,3-Bis(palmitoyloxy)-(2-RS)-propyl]-N-palmitoyl-(R)-Cys-Ser-Lys₄-OH (Pam3Cys) and polyinosinic:polycytidylic acid (poly I:C; VacciGrade) was purchased from InvivoGen. Purified Adenylate Cyclase Toxin (AC) from *Bordetella pertussis* was a gift of E. Hewlett (Univ. of Virginia) and has been described previously³⁹. The mPGES inhibitor (CAY10526) was obtained from Cayman Chemical. PGE₂, EP4 antagonist (BGC 20–1531), EP2 antagonist (PF-04418948), EP3 antagonist (L-798,106), AKT1&2 inhibitor (AKTi-1/2), PKA inhibitor (H89 dihydrochloride), and EPAC inhibitor (ESI 09) were obtained from Tocris Bioscience.

ELISA

The ELISA used to detect PGE₂ was purchased from ENZO and used according to manufacturers' instructions. The murine IFN- β ELISA was performed as previously described³⁵.

Bacterial Strains and infections

Salmonella Typhimurium (*ST*) strain SL1344 was a kind gift of R.Ernst. Enterohemorrhagic *E. coli* (EHEC) serotype O157:H7 strain TUV93–0 (EDL933 *stx*), enteropathogenic *E. coli* (EPEC) serotype O127:H6 strain E2348/69, and *Citrobacter rodentium* strain ICC168 have been previously described^{66, 67, 68}, and were kindly provided by J. B. Kaper. *In vitro* infections of murine peritoneal macrophages with *ST* were carried out as described

previously¹⁷. Briefly, a single colony of *ST* strain SL1344 was inoculated into 5 ml LB media and grown overnight at 37 °C with shaking. The following morning, an additional 10 ml LB media was inoculated with 200 µl overnight culture and incubated at 37° C with shaking until OD₆₀₀ reached 1.5. One ml of culture was pelleted by centrifugation and re-suspended into 1 ml sterile PBS. A quantity amounting to 400 µl bacterial suspension was mixed with 600 µl sterile PBS to obtain a concentration of $\sim 4 \times 10^6$ bacteria per 10 ml culture. An appropriate volume of this re-suspension was mixed with 37 °C antibiotic-free RPMI 1640 to obtain the desired MOI. Bacteria were added to macrophages in culture plates, and infections were synchronized by centrifugation for 5 min at 700 rpm. Infected cultures were incubated at 37° C for 30 min, and the infection media was removed and replaced with RPMI 1640 containing 50 µg/ml gentamicin and incubated for an additional 45 min at 37° C to kill extracellular bacteria. Following gentamicin incubation, media was removed, the cultures were washed twice with sterile PBS, and the media replaced with antibiotic-free RPMI 1640.

For *in vitro* EHEC, EPEC, and *Citrobacter rodentium* infections, TEPM monolayers (9×10^5 cells/well) were plated 24 h prior to infection. Bacteria were inoculated directly from glycerol stocks in 3 ml of L-broth medium and grown overnight at 37° C without shaking. Macrophage monolayers were infected with each of the strains in triplicate at an MOI = 25 (2.3×10^7 bacteria/well) in 1 ml RPMI 1640 media containing 2% FBS. Control monolayers were added 1 ml of media only. The monolayers were incubated for 1 h at 37 °C in 7% CO₂. The medium was then replaced with 1 ml of fresh media containing 100 µg/ml gentamycin and 10µM CAY10526 (for drug-treated samples), and cells were incubated for an additional 6 h.

For *in vivo* *ST* infection experiments to measure cytokine expression, wild-type C57BL/6J mice were pre-treated by i.p. injection with saline or BGC201531 (50 µg) and after 60 min, mice were infected i.p. as described previously¹⁷. *ST*-infected mice were sacrificed 8 h later and the spleens and livers harvested for gene expression analysis. For *in vivo* *ST* lethality studies, mice were given a single i.p. injection of BGC201531 (50 µg) one hour prior to i.p. infection with 1×10^3 *ST*. On each successive day, animals were given injections of BGC20–1531 (50 µg) twice daily and monitored for morbidity and mortality.

Macrophage Stimulation

TEPM or BMDM were plated at 2×10^6 cells/well in 12-well plates and allowed to rest overnight. Macrophage cultures were pre-treated for 30 min with vehicle or inhibitor, followed by stimulation with LPS (100 ng/ml) or Pam3Cys (InvivoGen) (250 ng/ml) for the indicated times.

Measurement of Macrophage Viability

Macrophage viability was assessed using the Cell Titer Glo 2 reagent from Promega according to manufacturer's instructions.

Immunoblot

Whole cell lysates from macrophage cultures were obtained by the addition of lysis buffer (20 mM HEPES pH6.8, 1.0% TRITON X-100, 0.1% SDS, 150 mM NaCl, 10 mM NaF, 1 mM PMSF) and subsequent incubation at 4° C. Cell lysates were separated by electrophoresis in a denaturing SDS-PAGE gel and subsequent transfer to PVDF membrane. Blots were incubated overnight in relevant primary antibodies at 4 °C and washed 3× with PBS, and then incubated with appropriate HRP-conjugated secondary antibody (Jackson Immunochemicals). Blots were developed following incubation in ECL PLUS Western Blotting Detection Reagent (Amersham Bioscience). Immunoblots were quantitated using Image J software (NIH), and the ratio of specific signal intensity to loading control for each lane is provided directly under each blot.

TLR4 internalization assay

These experiments were carried out in sterile flow cytometry tubes (BD). TEPM were rested overnight, pretreated with medium only, BGC 20–1531, CAY10526, or synthetic PGE₂ for 15 min. To stimulate TLR4 internalization, cells were treated with LPS (100 ng/mL) at 37 °C, with 5% CO₂. Sample collection and staining were performed as previously described by Zanoni et al.⁷, with minor modifications⁶⁹. Briefly, at 0, 30, 60, and 90 min after addition of LPS, cells were rapidly cooled by adding 2 volumes of ice-cold FACS buffer (0.5 % FBS + 2.0 mM EDTA in PBS), centrifuged (1200 rpm) in a pre-chilled centrifuge, and resuspended in 0.5 ml/10⁶ cells of ice-cold media. Samples were stored on ice until the collection of the last time point. All subsequent steps were carried out on ice using ice-cold buffers and reagents. Cells were washed twice in FACS buffer, treated with anti-CD16/32 (FcγRII-blocking antibody; 2.0 μg/10⁶ cells) for 20 min, and stained with PE-conjugated anti-mouse CD284 (anti-TLR4 antibody; 0.4 μg/10⁶ cells) or PE-conjugated rat IgG2a, κ isotype control (all from BioLegend) for 30 min in the dark. Cells were washed twice in FACS buffer and read within 30 min on a FACS Canto II Flow Cytometer (BD) using FACS Diva software (BD) in the University of Maryland Flow Cytometry Core Facility, Center for Innovative Biomedical Resources (CIBR), collecting 10⁴ single cell events per tube. To confirm the viability of cells after flow cytometry, a sample of the cells remaining after completion of flow cytometry was stained with 0.2% trypan blue solution (Sigma) and live and total cell counts were determined by counting unstained and all cells, respectively, using a standard hemocytometer (Reichert). Graphing and statistical analysis of FCS3 files was carried out in FCS Express 6 Plus (DeNovo Software). Data are expressed as the average mean fluorescence intensity at each time point.

Caspase 1 and Caspase 8 activation assays.

To measure Caspase 1 activation, TEPM were plated at 2×10^6 per well in 12-well plates. Cells were then treated with vehicle or EP4 antagonist (50 μM) for 30 min followed by LPS (100 ng/ml) for 3 or 6 h. For positive control conditions, 5 mM ATP (SigmaAldrich) was added to cultures for the final 30 min. Whole cell lysates were probed with antibody against Caspase 1. For Caspase 8 activation, macrophages were pretreated with inhibitors for 30 min prior to stimulation with LPS for the indicated times. Whole cell lysates were probed with antibodies against Caspase 8 p55 (Enzo) or p18 (Cell Signaling).

Quantitative real-time RT-PCR

Total mRNA was isolated from TEPM or BMDM using TRIzol (Invitrogen, Carlsbad, CA) reagent, according to manufacturer's instructions. A total of 1 µg RNA was used in oligo(dT) cDNA synthesis (Bio-Rad RT system). Quantitative RT-PCR (qRT-PCR) was carried out using an ABI Prism 7900HT Sequence Detection System (Applied Biosystems) utilizing SYBR Green reagent (Applied Biosystems) and transcript-specific primers. mRNA expression values were normalized to those of the housekeeping gene *Hprt* in each sample, and the fold-change in expression was calculated by the 2^{-Ct} method⁷⁰.

Generation of microarray data and bioinformatics.

Wild-type C57BL/6J and *Ifnb*^{-/-} TEPMs were mock-infected or infected with *ST* (MOI = 4) for 6 h. Total RNA was purified with Roche HiPure kit according to instructions. RNA was hybridized to Affymetrix GeneChip 2.0 mouse total transcriptome arrays at the UMB Center for innovative Biomedical Resources. Genes displaying a greater than two-fold differential expression in the *Ifnb*^{-/-} background were used for Upstream Regulator Analytic in the Ingenuity Pathway Assist software (Promega).

Statistics

All data were analyzed using GraphPad Prism (v.5.0) software. Data are presented as arithmetic means with error bars, which reflect standard error of the mean (SEM) as indicated. Where relevant, the sample size is indicated in the figure legends. Statistical significance was determined using Student's *t* test (two-tailed) except for (6e) where a Mantel-Cox test was used. A *P* value of less than 0.05 was considered statistically significant

Supplementary Material

Refer to Web version on PubMed Central for supplementary material.

Acknowledgments

We would like to gratefully acknowledge R. Rajaiah (University of Mysore, India) for technical assistance with the TLR4 internalization assay and J.C. Blanco (Sigmovir Biosystems, Inc.) and D. Prantner (UMB) for their helpful critiques of this manuscript. Flow cytometry and microarray analyses were performed at the Center for Innovative Biomedical Resources (CIBR) at the University of Maryland, School of Medicine. This work was supported by NIH grants AI123371 and AI125215 (SNV), as well as AR061491 (BK).

References

1. Medzhitov R, Preston-Hurlburt P & Janeway CA, Jr. A human homologue of the Drosophila Toll protein signals activation of adaptive immunity. *Nature* 388, 394–397 (1997). [PubMed: 9237759]
2. Poltorak A et al. Defective LPS signaling in C3H/HeJ and C57BL/10ScCr mice: mutations in Tlr4 gene. *Science* 282, 2085–2088 (1998). [PubMed: 9851930]
3. Shimazu R et al. MD-2, a molecule that confers lipopolysaccharide responsiveness on Toll-like receptor 4. *The Journal of experimental medicine* 189, 1777–1782 (1999). [PubMed: 10359581]
4. Brubaker SW, Bonham KS, Zanoni I & Kagan JC Innate immune pattern recognition: a cell biological perspective. *Annu Rev Immunol* 33, 257–290 (2015). [PubMed: 25581309]

5. Bryant CE, Symmons M & Gay NJ Toll-like receptor signalling through macromolecular protein complexes. *Mol Immunol* 63, 162–165 (2015). [PubMed: 25081091]
6. Kagan JC et al. TRAM couples endocytosis of Toll-like receptor 4 to the induction of interferon-beta. *Nature immunology* 9, 361–368 (2008). [PubMed: 18297073]
7. Zanoni I et al. CD14 controls the LPS-induced endocytosis of Toll-like receptor 4. *Cell* 147, 868–880 (2011). [PubMed: 22078883]
8. Jiang Z et al. CD14 is required for MyD88-independent LPS signaling. *Nature immunology* 6, 565–570 (2005). [PubMed: 15895089]
9. Fitzgerald KA et al. IKKepsilon and TBK1 are essential components of the IRF3 signaling pathway. *Nature immunology* 4, 491–496 (2003). [PubMed: 12692549]
10. Fitzgerald KA et al. LPS-TLR4 signaling to IRF-3/7 and NF-kappaB involves the toll adapters TRAM and TRIF. *The Journal of experimental medicine* 198, 1043–1055 (2003). [PubMed: 14517278]
11. Yamamoto M et al. Role of adaptor TRIF in the MyD88-independent toll-like receptor signaling pathway. *Science* 301, 640–643 (2003). [PubMed: 12855817]
12. Yamamoto M et al. TRAM is specifically involved in the Toll-like receptor 4-mediated MyD88-independent signaling pathway. *Nature immunology* 4, 1144–1150 (2003). [PubMed: 14556004]
13. Maelfait J et al. Stimulation of Toll-like receptor 3 and 4 induces interleukin-1beta maturation by caspase-8. *The Journal of experimental medicine* 205, 1967–1973 (2008). [PubMed: 18725521]
14. He S, Liang Y, Shao F & Wang X Toll-like receptors activate programmed necrosis in macrophages through a receptor-interacting kinase-3-mediated pathway. *Proceedings of the National Academy of Sciences of the United States of America* 108, 20054–20059 (2011). [PubMed: 22123964]
15. Moriwaki K, Bertin J, Gough PJ & Chan FK A RIPK3-caspase 8 complex mediates atypical pro-IL-1beta processing. *Journal of immunology* 194, 1938–1944 (2015).
16. Casanova JL, Abel L & Quintana-Murci L Human TLRs and IL-1Rs in host defense: natural insights from evolutionary, epidemiological, and clinical genetics. *Annu Rev Immunol* 29, 447–491 (2011). [PubMed: 21219179]
17. Perkins DJ et al. Salmonella Typhimurium Co-opts the Host Type I IFN System To Restrict Macrophage Innate Immune Transcriptional Responses Selectively. *Journal of immunology* 195, 2461–2471 (2015).
18. Deriu E et al. Influenza Virus Affects Intestinal Microbiota and Secondary Salmonella Infection in the Gut through Type I Interferons. *PLoS Pathog* 12, e1005572 (2016). [PubMed: 27149619]
19. Henry T et al. Type I IFN signaling constrains IL-17A/F secretion by gammadelta T cells during bacterial infections. *Journal of immunology* 184, 3755–3767 (2010).
20. Mayer-Barber KD et al. Innate and adaptive interferons suppress IL-1alpha and IL-1beta production by distinct pulmonary myeloid subsets during Mycobacterium tuberculosis infection. *Immunity* 35, 1023–1034 (2011). [PubMed: 22195750]
21. Rayamajhi M, Humann J, Penheiter K, Andreasen K & Lenz LL Induction of IFN-1alpha enables Listeria monocytogenes to suppress macrophage activation by IFN-gamma. *The Journal of experimental medicine* 207, 327–337 (2010). [PubMed: 20123961]
22. Heyninck K & Beyaert R A20 inhibits NF-kappaB activation by dual ubiquitin-editing functions. *Trends Biochem Sci* 30, 1–4 (2005). [PubMed: 15653317]
23. Ma A & Malynn BA A20: linking a complex regulator of ubiquitylation to immunity and human disease. *Nat Rev Immunol* 12, 774–785 (2012). [PubMed: 23059429]
24. Turer EE et al. Homeostatic MyD88-dependent signals cause lethal inflammation in the absence of A20. *The Journal of experimental medicine* 205, 451–464 (2008). [PubMed: 18268035]
25. Buczynski MW et al. TLR-4 and sustained calcium agonists synergistically produce eicosanoids independent of protein synthesis in RAW264.7 cells. *The Journal of biological chemistry* 282, 22834–22847 (2007). [PubMed: 17535806]
26. Hessle CC, Andersson B & Wold AE Gram-negative, but not Gram-positive, bacteria elicit strong PGE2 production in human monocytes. *Inflammation* 27, 329–332 (2003). [PubMed: 14760940]

27. Moore RN, Urbaschek R, Wahl LM & Mergenhagen SE Prostaglandin regulation of colony-stimulating factor production by lipopolysaccharide-stimulated murine leukocytes. *Infection and immunity* 26, 408–414 (1979). [PubMed: 397926]
28. Bowman CC & Bost KL Cyclooxygenase-2-mediated prostaglandin E2 production in mesenteric lymph nodes and in cultured macrophages and dendritic cells after infection with *Salmonella*. *Journal of immunology* 172, 2469–2475 (2004).
29. Mayer-Barber KD et al. Host-directed therapy of tuberculosis based on interleukin-1 and type I interferon crosstalk. *Nature* 511, 99–103 (2014). [PubMed: 24990750]
30. Dennis EA & Norris PC Eicosanoid storm in infection and inflammation. *Nat Rev Immunol* 15, 511–523 (2015). [PubMed: 26139350]
31. von Moltke J et al. Rapid induction of inflammatory lipid mediators by the inflammasome in vivo. *Nature* 490, 107–111 (2012). [PubMed: 22902502]
32. Boulet L et al. Deletion of microsomal prostaglandin E2 (PGE2) synthase-1 reduces inducible and basal PGE2 production and alters the gastric prostanoid profile. *The Journal of biological chemistry* 279, 23229–23237 (2004). [PubMed: 15016822]
33. Sugimoto Y & Narumiya S Prostaglandin E receptors. *The Journal of biological chemistry* 282, 11613–11617 (2007). [PubMed: 17329241]
34. Mortimer L, Moreau F, MacDonald JA & Chadee K NLRP3 inflammasome inhibition is disrupted in a group of auto-inflammatory disease CAPS mutations. *Nature immunology* 17, 1176–1186 (2016). [PubMed: 27548431]
35. Roberts ZJ et al. The chemotherapeutic agent DMXAA potently and specifically activates the TBK1-IRF-3 signaling axis. *The Journal of experimental medicine* 204, 1559–1569 (2007). [PubMed: 17562815]
36. Hoebe K et al. Identification of Lps2 as a key transducer of MyD88-independent TIR signalling. *Nature* 424, 743–748 (2003). [PubMed: 12872135]
37. Zanoni I et al. CD14 controls the LPS-induced endocytosis of Toll-like receptor 4. *Cell* 147, 868–880 (2011). [PubMed: 22078883]
38. Konya V, Marsche G, Schuligoi R & Heinemann A E-type prostanoid receptor 4 (EP4) in disease and therapy. *Pharmacol Ther* 138, 485–502 (2013). [PubMed: 23523686]
39. Perkins DJ, Gray MC, Hewlett EL & Vogel SN *Bordetella pertussis* adenylate cyclase toxin (ACT) induces cyclooxygenase-2 (COX-2) in murine macrophages and is facilitated by ACT interaction with CD11b/CD18 (Mac-1). *Mol Microbiol* 66, 1003–1015 (2007). [PubMed: 17927697]
40. Zaslona Z et al. The Induction of Pro-IL-1beta by Lipopolysaccharide Requires Endogenous Prostaglandin E2 Production. *Journal of immunology* 198, 3558–3564 (2017).
41. Robinson N et al. Type I interferon induces necroptosis in macrophages during infection with *Salmonella enterica* serovar Typhimurium. *Nature immunology* 13, 954–962 (2012). [PubMed: 22922364]
42. Stefan KL, Fink A, Surana NK, Kasper DL & Dasgupta S Type I interferon signaling restrains IL-10R+ colonic macrophages and dendritic cells and leads to more severe *Salmonella* colitis. *PLoS One* 12, e0188600 (2017). [PubMed: 29190678]
43. Kayagaki N et al. DUBA: a deubiquitinase that regulates type I interferon production. *Science* 318, 1628–1632 (2007). [PubMed: 17991829]
44. Jabir MS et al. Caspase-1 cleavage of the TLR adaptor TRIF inhibits autophagy and beta-interferon production during *Pseudomonas aeruginosa* infection. *Cell host & microbe* 15, 214–227 (2014). [PubMed: 24528867]
45. Bothwell W, Verburg M, Wynalda M, Daniels EG & Fitzpatrick FA A radioimmunoassay for the unstable pulmonary metabolites of prostaglandin E1 and E2: an indirect index of their in vivo disposition and pharmacokinetics. *J Pharmacol Exp Ther* 220, 229–235 (1982). [PubMed: 6948952]
46. Duffin R et al. Prostaglandin E(2) constrains systemic inflammation through an innate lymphoid cell-IL-22 axis. *Science* 351, 1333–1338 (2016). [PubMed: 26989254]
47. Fujino H, West KA & Regan JW Phosphorylation of glycogen synthase kinase-3 and stimulation of T-cell factor signaling following activation of EP2 and EP4 prostanoid receptors by prostaglandin E2. *The Journal of biological chemistry* 277, 2614–2619 (2002). [PubMed: 11706038]

48. Jing H, Vassiliou E & Ganea D Prostaglandin E2 inhibits production of the inflammatory chemokines CCL3 and CCL4 in dendritic cells. *Journal of leukocyte biology* 74, 868–879 (2003). [PubMed: 12960284]
49. Kunkel SL et al. Prostaglandin E2 regulates macrophage-derived tumor necrosis factor gene expression. *The Journal of biological chemistry* 263, 5380–5384 (1988). [PubMed: 3162731]
50. Xu XJ, Reichner JS, Mastrofrancesco B, Henry WL, Jr. & Albina JE Prostaglandin E2 suppresses lipopolysaccharide-stimulated IFN-beta production. *Journal of immunology* 180, 2125–2131 (2008).
51. Husebye H et al. The Rab11a GTPase controls Toll-like receptor 4-induced activation of interferon regulatory factor-3 on phagosomes. *Immunity* 33, 583–596 (2010). [PubMed: 20933442]
52. Van Acker T et al. The small GTPase Arf6 is essential for the Tram/Trif pathway in TLR4 signaling. *The Journal of biological chemistry* 289, 1364–1376 (2014). [PubMed: 24297182]
53. Guichard A et al. Cholera toxin disrupts barrier function by inhibiting exocyst-mediated trafficking of host proteins to intestinal cell junctions. *Cell host & microbe* 14, 294–305 (2013). [PubMed: 24034615]
54. Guichard A et al. Anthrax toxins cooperatively inhibit endocytic recycling by the Rab11/Sec15 exocyst. *Nature* 467, 854–858 (2010). [PubMed: 20944747]
55. Guichard A, Nizet V & Bier E RAB11-mediated trafficking in host-pathogen interactions. *Nat Rev Microbiol* 12, 624–634 (2014). [PubMed: 25118884]
56. Guichard A et al. Anthrax edema toxin disrupts distinct steps in Rab11-dependent junctional transport. *PLoS Pathog* 13, e1006603 (2017). [PubMed: 28945820]
57. Castiglia V et al. Type I Interferon Signaling Prevents IL-1beta-Driven Lethal Systemic Hyperinflammation during Invasive Bacterial Infection of Soft Tissue. *Cell host & microbe* 19, 375–387 (2016). [PubMed: 26962946]
58. Auerbuch V, Brockstedt DG, Meyer-Morse N, O’Riordan M & Portnoy DA Mice lacking the type I interferon receptor are resistant to *Listeria monocytogenes*. *The Journal of experimental medicine* 200, 527–533 (2004). [PubMed: 15302899]
59. Nagarajan UM et al. Type I interferon signaling exacerbates *Chlamydia muridarum* genital infection in a murine model. *Infection and immunity* 76, 4642–4648 (2008). [PubMed: 18663004]
60. Dobrovolskaia MA et al. Induction of in vitro reprogramming by Toll-like receptor (TLR)2 and TLR4 agonists in murine macrophages: effects of TLR “homotolerance” versus “heterotolerance” on NF-kappa B signaling pathway components. *Journal of immunology* 170, 508–519 (2003).
61. Shirey KA et al. The anti-tumor agent, 5,6-dimethylxanthenone-4-acetic acid (DMXAA), induces IFN-beta-mediated antiviral activity in vitro and in vivo. *Journal of leukocyte biology* 89, 351–357 (2011). [PubMed: 21084628]
62. Facemire CS et al. A major role for the EP4 receptor in regulation of renin. *Am J Physiol Renal Physiol* 301, F1035–1041 (2011). [PubMed: 21835766]
63. Nguyen M et al. The prostaglandin receptor EP4 triggers remodelling of the cardiovascular system at birth. *Nature* 390, 78–81 (1997). [PubMed: 9363893]
64. Richard K, Vogel SN & Perkins DJ Type I interferon licenses enhanced innate recognition and transcriptional responses to *Francisella tularensis* live vaccine strain. *Innate Immun* 22, 363–372 (2016). [PubMed: 27231145]
65. McIntire FC, Sievert HW, Barlow GH, Finley RA & Lee AY Chemical, physical, biological properties of a lipopolysaccharide from *Escherichia coli* K-235. *Biochemistry* 6, 2363–2372 (1967). [PubMed: 4867999]
66. Barthold SW, Coleman GL, Bhatt PN, Osbaldiston GW & Jonas AM The etiology of transmissible murine colonic hyperplasia. *Lab Anim Sci* 26, 889–894 (1976). [PubMed: 1018473]
67. Donohue-Rolfe A, Kondova I, Oswald S, Hutto D & Tzipori S *Escherichia coli* O157:H7 strains that express Shiga toxin (Stx) 2 alone are more neurotropic for gnotobiotic piglets than are isotypes producing only Stx1 or both Stx1 and Stx2. *J Infect Dis* 181, 1825–1829 (2000). [PubMed: 10823794]
68. Levine MM et al. *Escherichia coli* strains that cause diarrhoea but do not produce heat-labile or heat-stable enterotoxins and are non-invasive. *Lancet* 1, 1119–1122 (1978). [PubMed: 77415]

69. Rajaiah R, Perkins DJ, Ireland DD & Vogel SN CD14 dependence of TLR4 endocytosis and TRIF signaling displays ligand specificity and is dissociable in endotoxin tolerance. *Proceedings of the National Academy of Sciences of the United States of America* 112, 8391–8396 (2015). [PubMed: 26106158]
70. Livak KJ & Schmittgen TD Analysis of relative gene expression data using real-time quantitative PCR and the 2(-Delta Delta C(T)) Method. *Methods* 25, 402–408 (2001). [PubMed: 11846609]

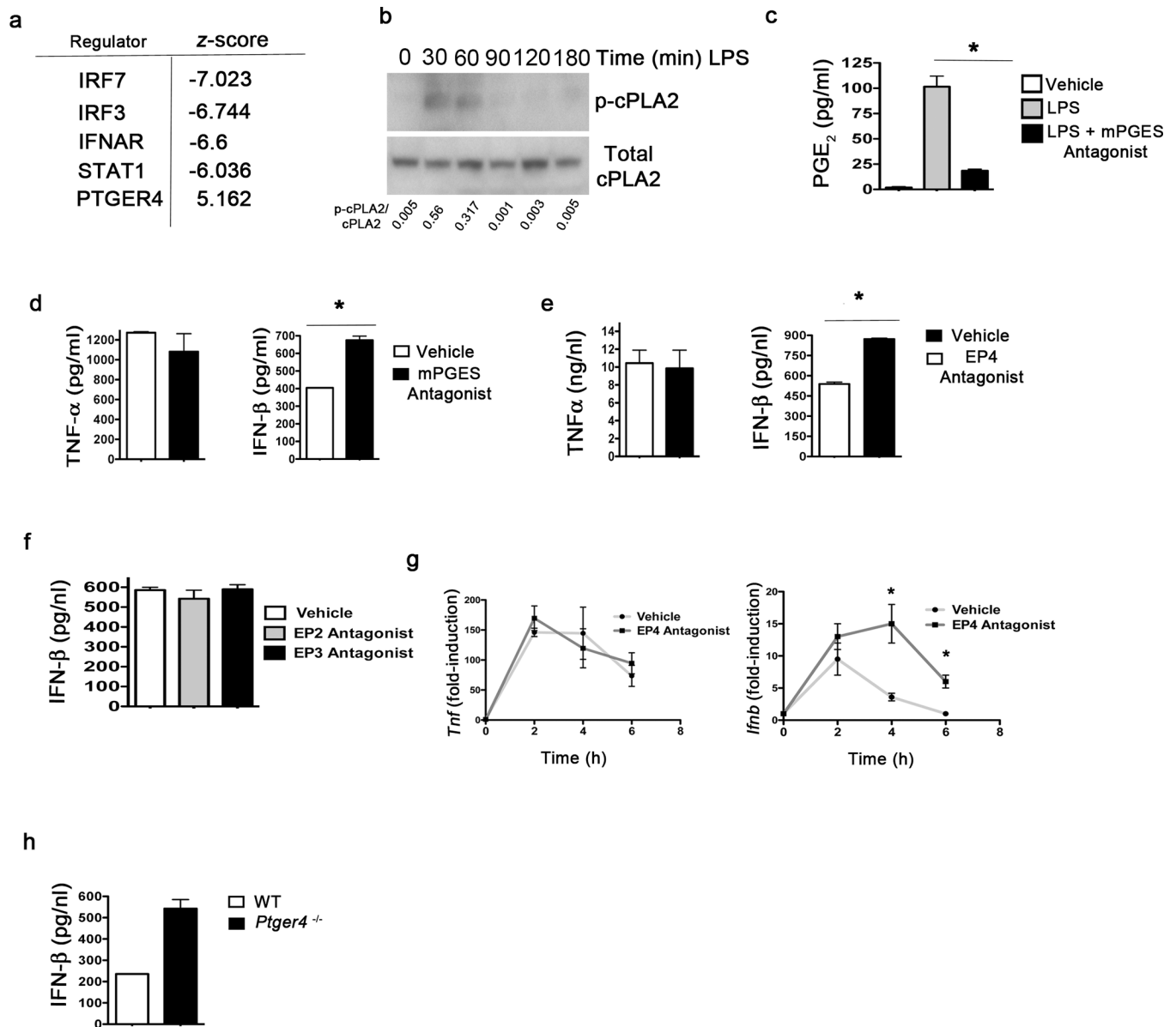


Figure 1. Rapid LPS-dependent PGE₂ limits TLR4-mediated IFN- β production.

(a) Table showing a partial list of transcriptional regulators with predicted differential activity in *ST*-infected *Ifnb*^{-/-} versus WT primary murine thioglycollate-elicited peritoneal macrophages (TEPM). (b) TEPM were stimulated with 100 ng/ml LPS for the indicated times and whole cell lysates used in Western blots probed with the indicated antibodies. Densitometry of individual lanes was carried out using Image J software (NIH) and normalized for loading. (c) TEPM were pre-treated with vehicle (DMSO) or the mPGES antagonist prior to stimulation with 100 ng/ml LPS for 3 h. Cell supernatants were collected and PGE₂ levels quantified by ELISA. *P = 0.0003 (d) TEPM were stimulated as in (c) for 6 h and cell supernatants analyzed for TNF (left panel) and IFN- β (right panel) by ELISA. * P = 0.0043. (e) TEPM were pretreated with vehicle (DMSO) or EP4 antagonist (BGC 20–1531; 50 μ M) for 15 min prior to stimulation with 100 ng/ml LPS. Cell supernatants were

collected 6 h later and analyzed for TNF and IFN- β by ELISA. * P = .02. (f) TEPM were pre-treated with vehicle (DMSO) or EP2 antagonist (PF-04418948; 50 μ M) or EP3 antagonist (L-798,106; 50- μ M) in DMSO for 30 min prior to stimulation with 100 ng/ml LPS for 6 h. Cell supernatants were collected and analyzed for IFN- β by ELISA. (g) TEPM pre-treated as in (e) were stimulated for the indicated times with 100 ng/ml LPS and total RNA collected for qRT-PCR quantitation. *P = .0024 (H) BMDMs generated from WT or *Ptger4*^{-/-} mice were stimulated for 6 h with 100 ng/ml LPS and supernatants analyzed for IFN- β by ELISA, *P=.002. For (a) analysis was carried out with expression data from three separate experiments (n=3). (b) is a representative image of at least four experiments (n>4). For (c-g) data are shown as mean \pm sem of n=3 independent experiments. Analysis carried out using a students (unpaired) t Test (two tailed). Experiments in (h) were carried out twice.

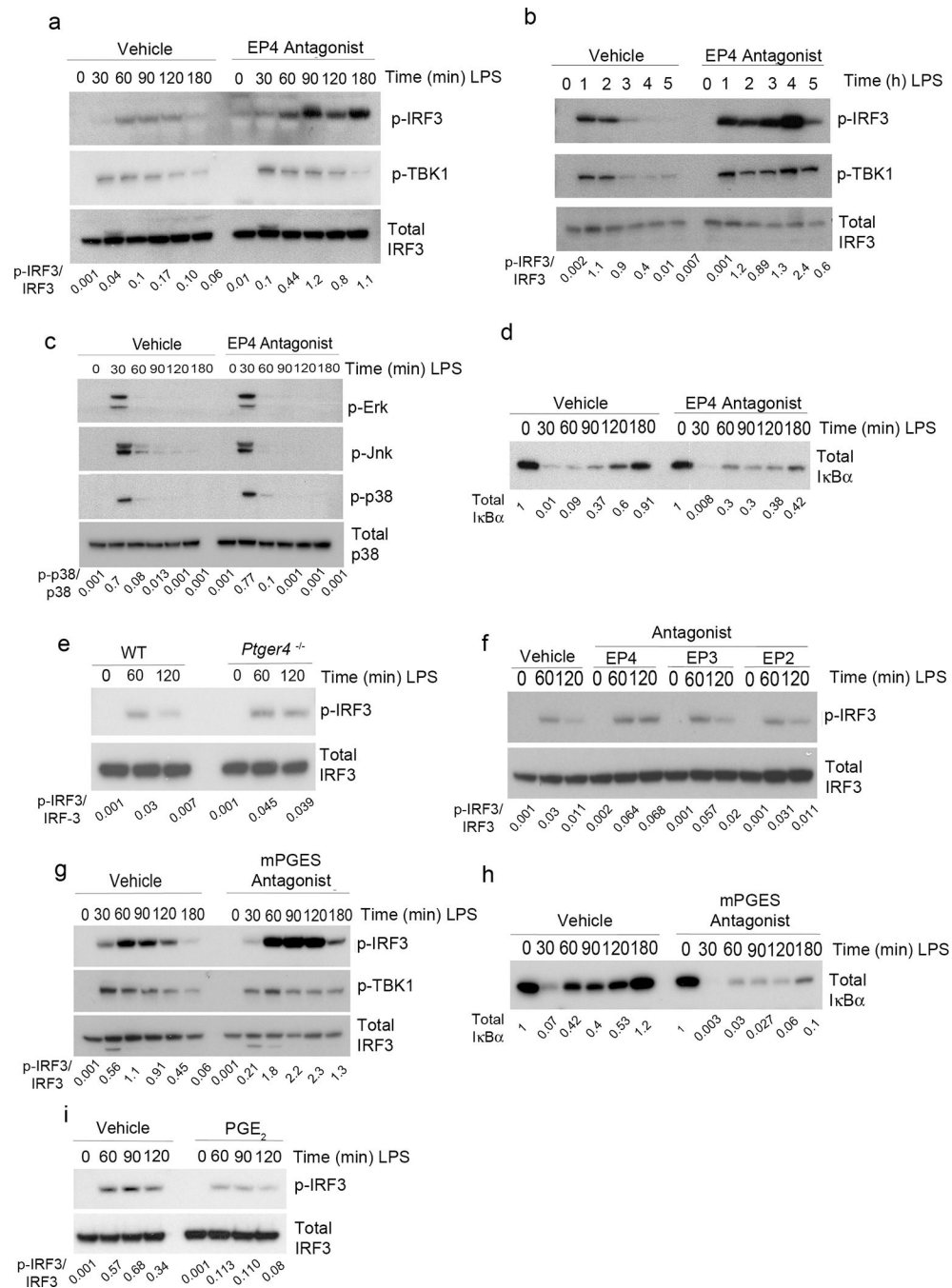


Figure 2. PGE₂ activation of EP4 receptor restricts IRF3 activation.

(a) TEPM were pre-treated with vehicle (DMSO) or EP4 antagonist as described in Figure 1 for 30 min prior to stimulation with 100 ng/ml LPS for the indicated times. Whole cell lysates were probed by Immunoblot analysis with the indicated antibodies. (b) TEPM were pre-treated as in (a) and stimulated with 100 ng/ml LPS for the indicated times. Whole cell lysates were probed as in (a) with the indicated antibodies. (c) Whole cell lysates from TEPM treated as in (a) were probed by immunoblot analysis with antibodies against MAPKs. (d) Whole cell lysates from TEPM treated as in (a) were probed by Immunoblot

analysis with antibodies against I κ B α . (e) BMDMs generated from *Ptger4*^{-/-} and littermate control femurs were stimulated with 100 ng/ml LPS for the indicated times and whole cell lysate probed by immunoblot analysis with indicated antibodies. (f) TEPM were pre-treated with DMSO or EP2- or EP3-specific receptor antagonists (50 μ M) for 30 min prior to stimulation with 100 ng/ml LPS for indicated times. Whole cell lysates were probed by immunoblot analysis with indicated antibodies. (g) TEPM were pretreated with DMSO or mPGES antagonist (CAY10526; 10 μ M) for 30 min prior to stimulation with 100 ng/ml LPS. Whole cell lysates were probed with the indicated antibodies. (h) Whole cell lysates from TEPM treated as in (G) were probed by with antibodies against I κ B α . (i) TEPM were pretreated with DMSO or PGE₂ (1 μ M) for 60 min prior to stimulation with 100 ng/ml LPS. Whole cell lysates were probed by immunoblot analysis with the indicated antibodies. For (a-d and g-i) experiments were carried out at least three separate times (n>3) with similar results and a representative image shown. For (e) experiments were carried out twice (n=2) with similar results.

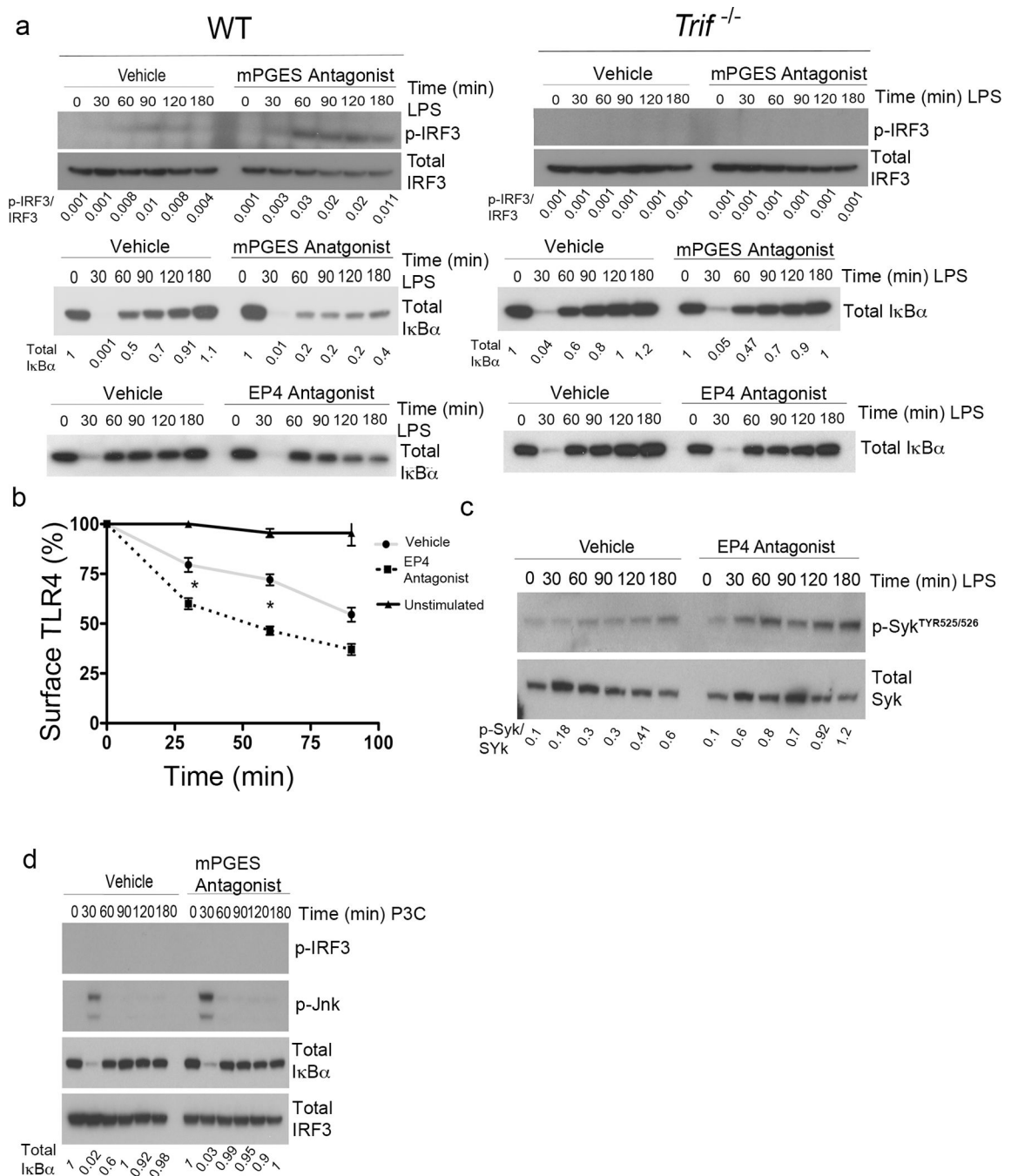


Figure 3. The PGE₂-EP4 axis regulates TLR4 signaling via the adapter TRIF.

(a) WT or *Trif*^{-/-} TEPM were pre-treated with vehicle (DMSO) or mPGES and/or EP4 antagonists, as indicated, for 30 min prior to stimulation with 100 ng/ml LPS. Whole cell lysates were harvested at indicated times for immunoblot analyses. In (A), activated and total IRF3, and total IκBα was similarly analyzed. (b) WT TEPM in FACS tubes were left unstimulated or were pre-treated with vehicle (DMSO) or EP4 antagonist for 15 min prior to stimulation with 100 ng/ml LPS. At the indicated time points, cells were placed on ice and then stained for cell surface TLR4, prior to being analyzed by Flow Cytometry. Figure

displays average mean fluorescent intensity at each time point. * $p < 0.05$ (c) WT TEPM treated as in (a) were harvested at indicated time points and whole cell lysates were probed by immunoblot analysis with the indicated anti-Syk antibodies. (d) TEPM were pre-treated as in (a) before being stimulated with 300 ng/ml P3C and then harvested for analysis by immunoblot analysis. For (a,c and d) experiments were carried out a minimum of three times ($n=3$) with similar results and a representative image is shown. For (b) $n=4$ independent experiments and data shown as mean \pm sem for each time point with analysis carried out by students (unpaired) t Test.

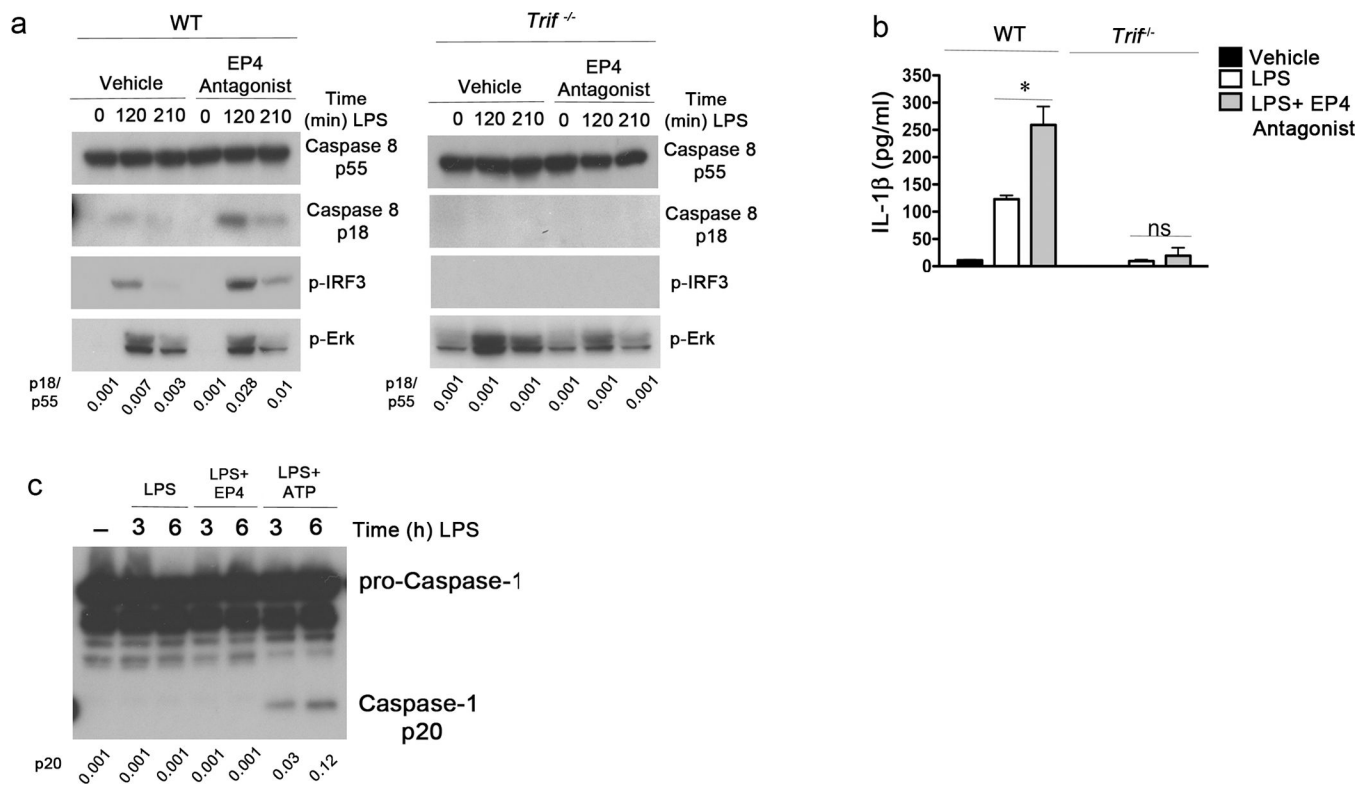


Figure 4. PGE₂-EP4 restricts LPS-induced, TRIF-dependent Caspase 8 activation and atypical IL-1 β processing.

(a) WT or *Trif*^{-/-} TEPM were pre-treated with DMSO or EP4 antagonist (50 μ M) for 30 min prior to stimulation with 100 ng/ml LPS for the indicated times. Whole cell lysates were probed by immunoblot analysis with the indicated antibodies. (b) WT or *Trif*^{-/-} TEPM were primed with 300 ng/ml Pam3Cys for 4 h, washed 2 \times in PBS, and the media replaced. Cells were subsequently stimulated with media alone or 100 ng/ml LPS with or without EP4 antagonist (50 μ M) for an additional 5 h. Cell supernatants were analyzed for mature IL-1 β by ELISA. *p=.005 (c) TEPM were stimulated for 3 or 6 h with LPS alone, or LPS and EP4 antagonist, or LPS for 3 and 6 h with 5 mM ATP added for the final 30 min. Whole cell lysates were probed by immunoblot analysis with antibody against caspase 1. For (a and c) experiments were carried out three separate times (n=3) with similar results and a representative image is shown. For (b) n= 3 separate experiments and data are shown as mean \pm sem with analysis carried out by students t Test (unpaired) (two tailed).

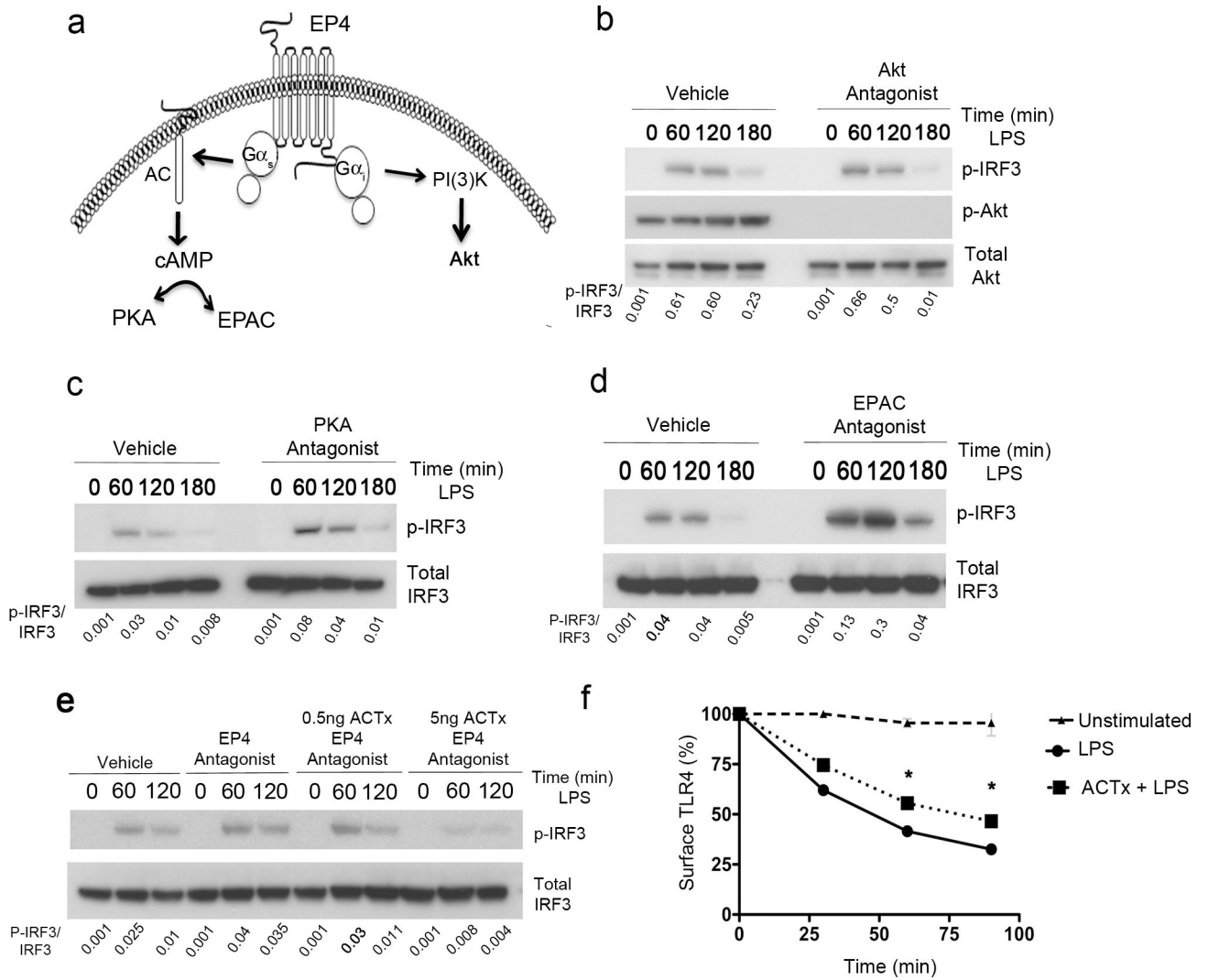


Figure 5. cAMP-dependent effectors are negative regulators of the TLR4-TRIF pathway.

(a) Model of signaling pathways downstream of EP4 receptor. (b-d) TEPM were pretreated with DMSO or Akt antagonist (AKTi; 10 μ M) (B), PKA antagonist (c) (H89 10 μ M), or EPAC antagonist (d) (ESI09 10 μ M), for 30 min prior to stimulation with 100 ng/ml LPS for the indicated times. Whole cell lysates were probed with the indicated anti-IRF3 antibodies. (e) TEPM were stimulated LPS and DMSO, LPS and EP4 antagonist, or LPS, EP4 antagonist and the indicated amount or recombinant purified Adenylate Cyclase Toxin. (f) TEPM treated as in (Figure 3b) were stimulated with LPS alone (100 ng/ml) or pre-incubated with 2.5 ng/ml purified ACTx for 30 min prior to addition of LPS and analyzed by flow cytometry for surface TLR4 P=.01. For (b-e), experiments were carried out a minimum of three separate times (n=3) with similar results and a representative blot shown. For (f) n=3 individual experiments and the data are shown as mean \pm sem.

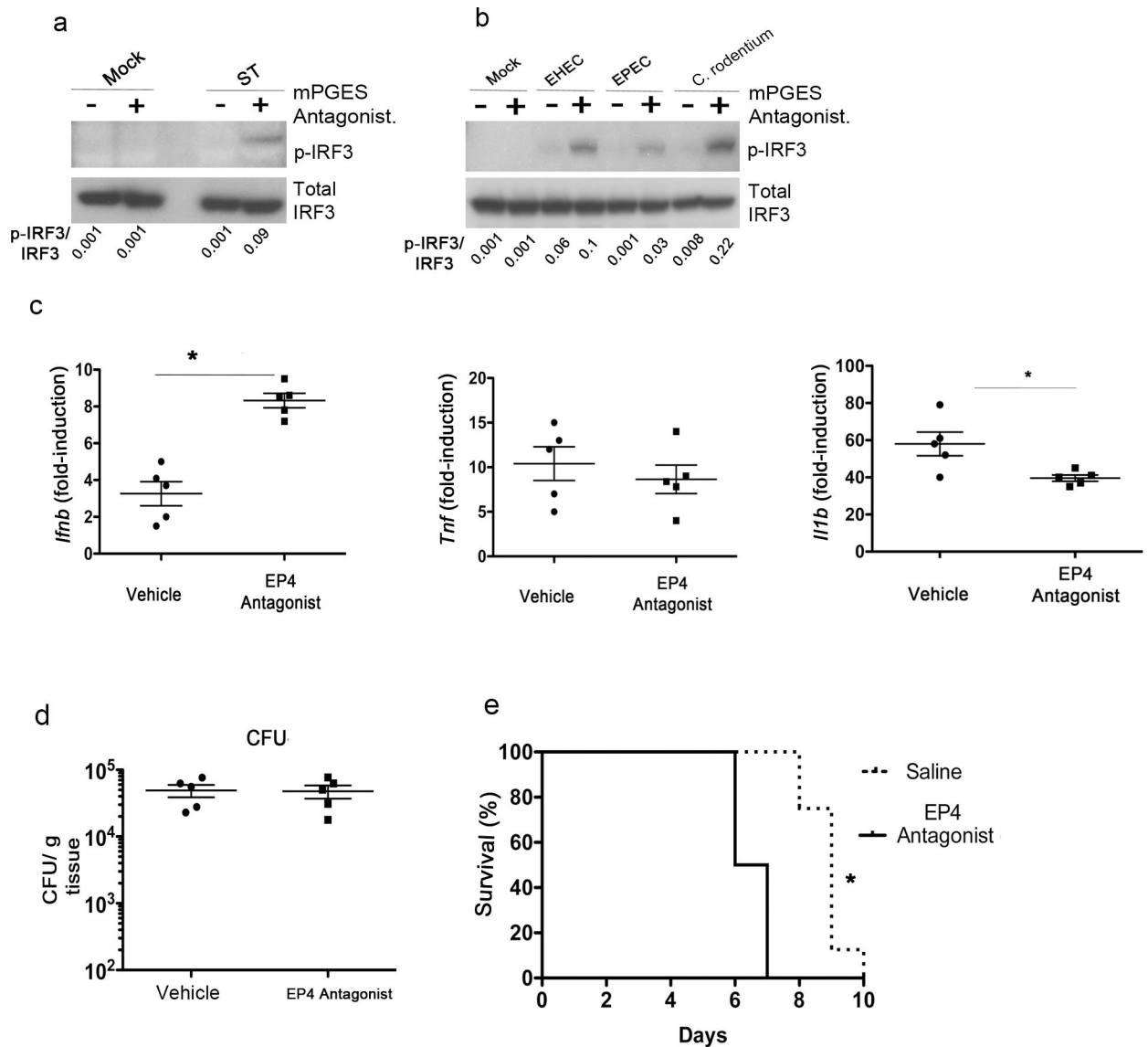


Figure 6. PGE₂ restricts IRF3 activation and IFN- β production in response to Gram negative pathogens *in vitro* and *in vivo*.

(a). TEPM were mock-infected or infected with *ST* (MOI = 4) for 30 min followed by gentamycin treatment and addition of mPGES antagonist (10 μ M). Infected and mock-infected TEPM were incubated for an additional 6 h and whole cell lysates harvested for immunoblot analysis with indicated antibodies. (b). TEPM were mock-infected or co-cultured with indicated strains (MOI = 25) for 60 min, followed by gentamycin and addition of mPGES antagonist (10 μ M). TEPM were incubated for additional 6 h before whole cell lysates were harvested for immunoblot analysis. (c) WT C57BL6/J (n=5) were pretreated by i.p. injection either with saline alone or with EP4 antagonist (50 μ g/mouse) 60 min prior to *ST* infection. All animals were infected i.p. with *ST* (1×10^8 /mouse) and 8 h later, mice were euthanized and spleen (shown) and liver harvested for gene expression analysis. Each point represents the response of an individual mouse. For *Ifnb**, p = .0017. For *Il1b** p = .023 (d) Animals were infected and treated as in (Figure 5C). At 8 h post-infection, spleens were

removed and viable bacteria enumerated by homogenization followed by serial dilution on streptomycin LB-agar plates. (e) Animals were given a single dose of saline or EP4 antagonist (50 µg/mouse) 1 h prior to i.p. infection with 1×10^3 ST. Each day subsequently animals were given twice daily injections of EP4 antagonist (50 µg/ mouse) or saline and monitored for morbidity and mortality. Analysis carried out by Mantel-Cox test. (one sided), * P= .001. For (a), experiments were carried out four separate times with similar results (n=4) and a representative images shown. For (b), experiments were carried out twice (n=2) with similar results and a representative image shown. For (c and d), the experiment was carried out with five individual animals per treatment group (n=5). For (e) n=10